



# Heat Release Rate of Heavy Goods Vehicle Fire in Tunnels with Fixed Water Based Fire-Fighting System

*M. K. Cheong\*, W. O. Cheong and K. W. Leong, Land Transport Authority, Singapore, Singapore*

*A. D. Lemaire and L. M. Noordijk, Efectis Nederland BV, Bleiswijk, The Netherlands*

**Abstract.** A series of large-scale fire tests for road tunnel application was conducted in a test tunnel facility in Spain. The aim of this fire tests program was to investigate the magnitude of the heat release rate generated by a fire in heavy goods vehicles (HGV's) with and without a fire suppression system in tunnels in Singapore; the possibility of interchanging a fire suppression system with other measures such as lowering the longitudinal flow velocity; and to acquire information on the appropriate design parameters (e.g., nozzle type, discharge density and activation time) to adopt based on the most probable fuel load used in these road tunnels. In order to ensure repeatability, simulated HGV's consisting of 228 pallets with 48 plastic pallets (20%) and 180 wooden pallets (80%) were used in all fire tests. An air velocity of approximately 3 m/s was applied. As the scope of work covered in this fire test program is very large, only the setup of the fire test and the findings on the effects of heat release rate with (Test 4) and without (Test 7) a fixed water based fire-fighting system are covered. The test results indicate that a substantial reduction of fire heat release rate can be obtained using a low-pressure deluge fire suppression system, as long as timely activation of the water is provided. However, the influence of the suppression system on CO production is significant. Such experimental data address the current dearth of knowledge on the actual effect of low-pressure deluge systems on the heat release rate from HGVs in tunnel fires.

**Keywords:** Heat release rate, Heavy goods vehicle fire, Fixed water based fire-fighting system, Low-pressure deluge

## Nomenclature

$E$	Heat of combustion per kmol of consumed oxygen (419.2 MJ/kmol of O <sub>2</sub> )
$E^{CO}$	Heat of combustion of CO per kmol of consumed oxygen (563.2 MJ/kmol of O <sub>2</sub> )
$M$	Molecular weight (kg/kmol)
$\dot{n}$	Molar flow rate (kmol/s)
$s$	Seconds (s)
$T$	Temperature (K)
Rh	Relative humidity (%)

\* Correspondence should be addressed to: M. K. Cheong, E-mail: mun\_kit\_cheong@lta.gov.sg

$\dot{q}$	Heat release rate (MW)
$X$	Mole fraction (unitless, corresponds to volume fraction for ideal gases)

### Superscripts

$e$	Exhaust conditions
$d$	Dry gas
$i$	Incoming air

### Subscripts

$CO$	Carbon monoxide
$CO_2$	Carbon dioxide
$H_2O$	Water
$N_2$	Nitrogen
$O_2$	Oxygen
$total$	Total (e.g. molar flow)

## 1. Introduction

A fire in a tunnel can be devastating and highly undesirable if not addressed in the early stages of fire development. This is particularly true for fires involving a heavy goods vehicle (HGV) carrying materials with high energy content. The resultant heat, soot and toxic combustible products can be produced more rapidly and therefore significantly increase the difficulty for escape, rescue and fire-fighting activities.

Over the past few years, there have been a number of large fire tests involving high energy content materials conducted in Europe. These tunnel fire test programs have provided better insight on fire development in tunnels, allowing tunnel designers to enhance fire safety provisions. In the Runehamar fire test series, the peak heat release rate recorded on a goods vehicle carrying high energy content materials can vary from 66.4 MW to 201.9 MW [1]. Similar high peak heat release rates of 128 MW [2] were observed in the EUREKA 499 fire test involving an HGV trailer carrying 2 t of furniture. The Runehamar and EUREKA 499 fire tests were conducted with no fixed water based fire-fighting system intervention and a tunnel air velocity of 3 m/s and 3 m/s to 6 m/s respectively.

These fire tests suggest that rapid heat release rate development could result in catastrophic consequences in the event of a fire in a tunnel. The outcome of these new findings has indirectly influenced the recommendation of higher design fire values for new road tunnel projects (e.g. 200 MW for HGV). However, this consideration does not yet account for trade-off effects in fire protection such as application of a fixed water based fire-fighting system.

A series of fire tests for road tunnels with and without a fixed water based fire-fighting system was conducted in 2012. The aim of this fire test program was (i) to measure heat release rate with and without a fixed water based fire-fighting system; (ii) to determine the possibility of interchanging a fixed water based fire-fighting system with other measures such as lowering the longitudinal flow velocity; (iii) to acquire information on the appropriate design parameters (e.g. nozzle type,

discharge density and activation time) to adopt based on the most probable fuel load used in specific road tunnels. A total of 10 laboratory fire tests and 7 large scale fire tests (refer to Table 1) was conducted in this fire test program.

## 2. Large-Scale Tunnel Fire Test

As the scope of work covered in this fire test series is very large, only the setup of each fire test and findings on the effect of heat release rate with (Test 4) and without (Test 7) a fixed water based fire-fighting system is covered here. Details of the tunnel geometry, suppression system used, fuel type and quantity are described in the following sections.

### 2.1. Tunnel Geometry and Ventilation System

The large-scale fire test was conducted in a test tunnel facility in Spain. It is a two lane road tunnel built in concrete, with a lower gallery for emergency and services, and three emergency exits (Figure 1a).

The length of the test tunnel is 600 m and the shape can be modified from a horseshoe shaped tunnel to a rectangular tunnel. For these large scale fire tests a rectangular test section is used. The minimum dimension of the rectangular test section is (at the location of the fire source) 7.3 m wide and 5.2 m high with a longitudinal gradient of 1% [3].

At the location of the fire source, walls are constructed inside the real test tunnel to protect the concrete against damage. The resulting cross-section is shown in the Figure 2a and b below. Jet fans at the southern end of the portal are used to generate an air velocity of 3 m/s in the tunnel for the entire duration of the fire test.

In the following section the position and labeling of all instrumentation is described.

**Table 1**  
**Large Scale Fire Test Schedule**

Test	Test description (variation)	Discharge density (mm/min)	Nozzle type	Activation time (min)	Fire in suppression zone
1	Directional nozzle	12	Dir 180°	4	Center of zone
2	Directional nozzle	8	Dir 180°	4	Center of zone
3	Standard spray nozzle	12	Standard	4	Center of zone
4	Standard spray nozzle <sup>a</sup>	12	Standard	4	Center of zone
5	Standard spray nozzle	12	Standard	4	End of zone
6	Standard spray nozzle	12	Standard	8	Center of zone
7	Unsuppressed	n.a.	n.a.	n.a.	Center of zone

<sup>a</sup> Test 4 is a repeat of Test 3; longitudinal ventilation rate in the tunnel was 2.8 m/s to 3 m/s

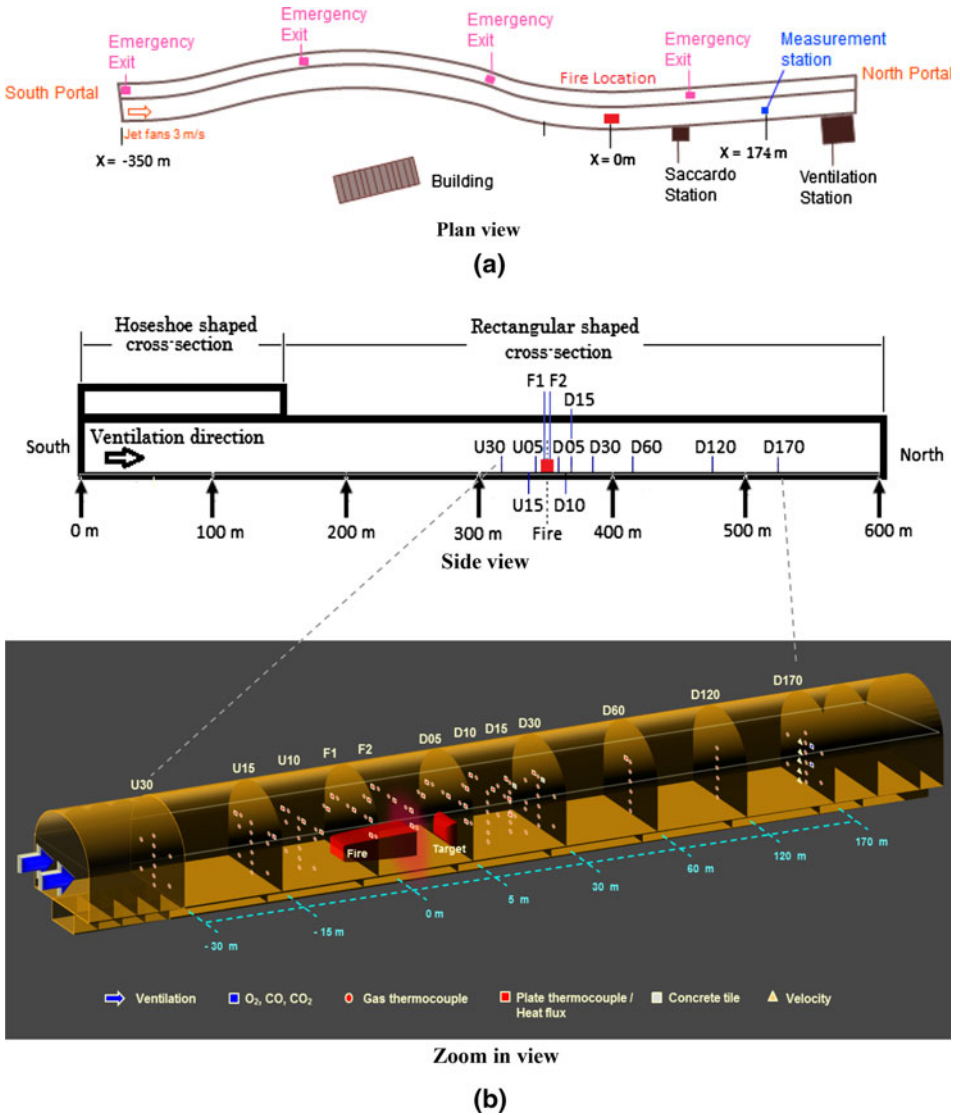


**Figure 1. (a) Plan view of the test tunnel showing the measurement station and fire location. (b) Overview of the test tunnel and positioning of sensors.**

*2.1.1. Tunnel Longitudinal Positions.* The longitudinal positions in the tunnel are defined relative to the fire source. The results presented are labeled according to the following three different areas (Figure 1b):

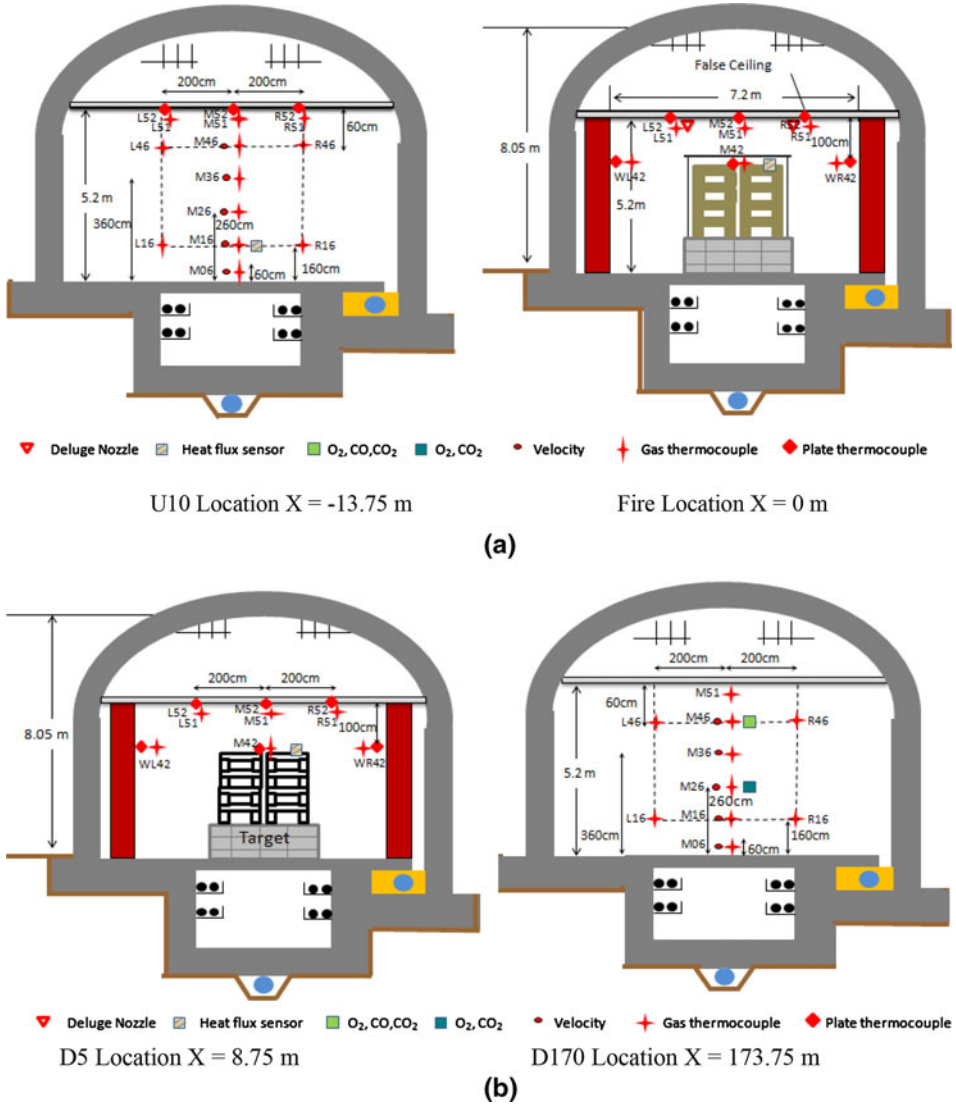


**Figure 2. (a, b) Cross-section of the test tunnel and instrumentation setup.**

- (I) *Upstream* The upstream edge of the fire source is defined as U0 and in the direction away from the fire source this value increases.  $U_x$  defines a position  $x$  m away from the upstream edge of the fire;
- (II) *Fire* The fire source is located between the upstream and downstream edge of the fire source. Positions in this area are denoted by F1 and F2;
- (III) *Downstream* The downstream edge of the fire source is defined as D0 and in the direction away from the fire source this value increases.  $D_x$  defines a position  $x$  m away from the downstream edge of the fire.

*2.1.2. Tunnel Cross-Section Positions.* The position of a sensor in a cross-section is denoted by the character sequences below:

- (I) *WL* on the wall on the left side;
- (II) *L* 2 m on the left of the centerline of the tunnel;
- (III) *M* on the centerline of the tunnel;
- (IV) *R* 2 m on the right of the centerline of the tunnel;
- (V) *WR* on the wall on the right side.

The height of a sensor in the tunnel is denoted with a 2 digit number combination relative to the floor of the tunnel. (An example: M51 means centerline of the tunnel at 5.1 m above floor level).

An overview of the instrumentation locations is shown in Figures 1b, 2a and b.

## **2.2. Fuel Quantity, Arrangement and Ignition Source**

In Singapore, there are regulations prohibiting vehicles carrying hazardous material from entering the road tunnels. To ensure the rules are followed, a Hazmat Transport Vehicle Tracking System (HTVTS) has been introduced by the Singapore Civil Defense Force (SCDF) [4]. The road traffic Act in Singapore also prohibits vehicles whose overall length (including any load) exceeds 13 m or trailers from entering the road tunnel [5]. Therefore, a typical rigid HGV fully loaded with pallets is a credible scenario to consider for the large scale fire test. The basic idea behind this configuration is an HGV fully loaded with pallets, as shown in Figure 3. The fire source consists of 228 pallets, with 48 plastic pallets (20%) and 180 wooden pallets (80%). The pallets are in 12 stacks, 19 pallets high on a 1 m elevation, with a steel frame around them that holds the steel top cover and a thin plastic tarpaulin on both sides of the fuel load. On the upstream and downstream sides of the pallet stack, a steel plate is mounted instead of the plastic tarpaulin. This setup is credible and realistic as it represents most typical cargo truck configurations. The pallets to be used are Euro pallet size with dimensions of 1.20 m  $\times$  0.80 m. The steel frame is constructed of hollow steel sections and the steel cover has a thickness of 1 mm.

The plastic pallets are distributed over the pallet stack consisting of 19 layers, starting with 4 layers of wooden pallets followed by 1 layer of plastic pallets. This stacking arrangement is repeated until the 15th layer followed with three layers of wooden pallets stacked on the 16 to 18th layers and plastic pallets in the remaining layer. Figures 4 and 5 show the placing of the pallets used in the fire tests. The fire source is ignited by two trays (0.35 m  $\times$  0.70 m) with each tray containing about 1 L of gasoline. The trays are positioned inside the two most upstream pallet stacks on the second pallet (Figure 5).

To assess the risk of fire spread to a position downstream, a target array consisting of two full pallet stacks is placed 5 m downstream from the rear end of the fire source (Figure 5).

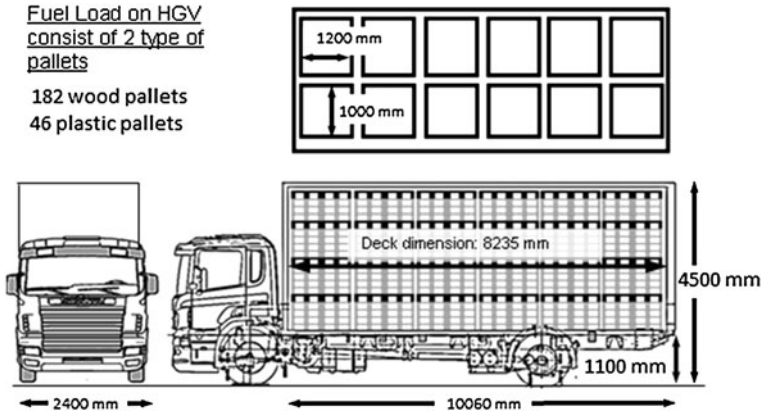


**Figure 3. Basic idea behind the configuration of the pallet stack.**

### 2.3. Suppression System and Instrumentation

There are various types of active fixed water based fire-fighting systems such as deluge systems, water spray systems, water mist systems and compressed air foam systems (CAF) considered or used for tunnel protection. The scope of this article is limited to deluge suppression systems with a low operating pressure (up to 5 bar) and a coverage area of at least 9 m<sup>2</sup> per nozzle. Two types of deluge nozzles are used in the fire test series: the pendant standard spray and directional 180° nozzles. These nozzle types are selected based on their proposed application for the Singapore road tunnel projects and the findings from the phase 1



**Figure 4. Photographs of fire load (left-before covering, center-as used in the fire test, upper right-target array and lower right-ignition tray).**

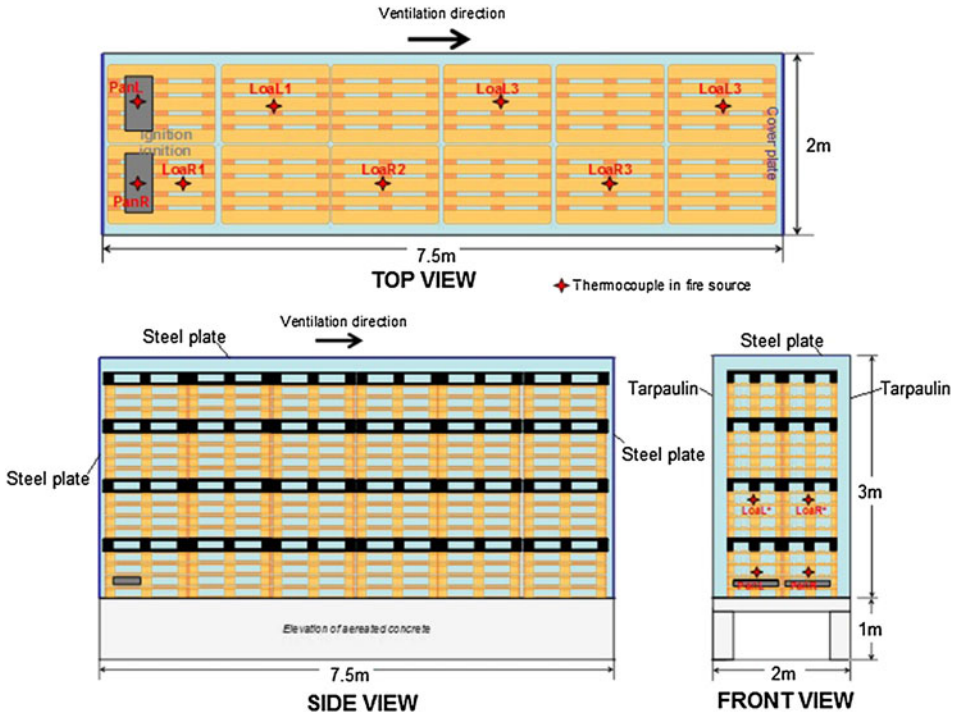


**Figure 5. Fuel load arrangement.**

laboratory fire tests, which examine sprinkler discharge density, nozzle type and the situation of a covered fire if the activation time of the system is critical for system effectiveness.

The deluge nozzles are shown in Figure 6. The difference between the standard spray nozzle and the 180° directional nozzle is the spray pattern, where the directional nozzle has more downward momentum and water discharge below the nozzle.

In the fire tests, the deluge system is designed to activate two zones simultaneously with a suppression zone of 25 m each. A total of 46 nozzles are used over an area of 50 m (length) by 7.2 m (width). Figure 7 shows a diagram of the deluge suppression system pipes at the ceiling for the large scale fire test program.

In the entire fire test series except in fire Test No. 6 (8 min activation) and no. 7 (free burning), an activation time of 4 min is used to activate the deluge system after fire detection. In these large scale fire tests, the detection system is simplified to just thermocouples located below the ceiling. The moment when any one of the thermocouples exceeds 60 °C represents detection; the deluge system will then be activated by manually turning on the deluge system after 4 min.



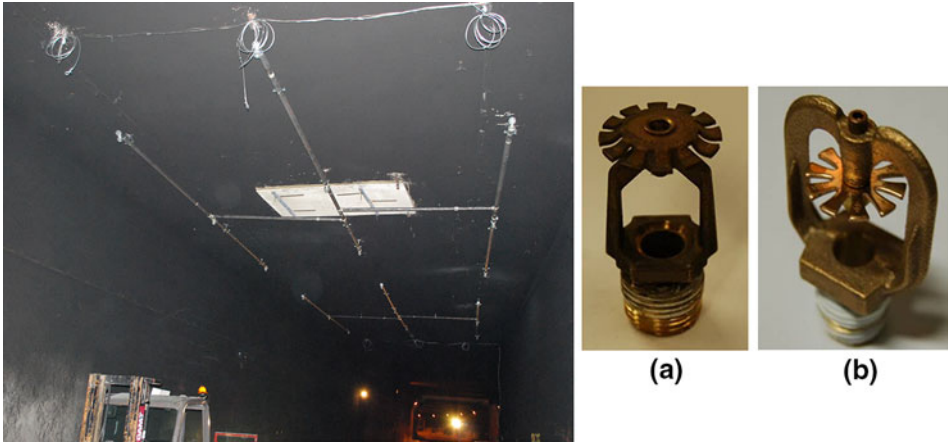


**Figure 6. Photograph of deluge suppression system pipes at the ceiling (left), standard spray (a) and directional 180° (b) nozzle.**

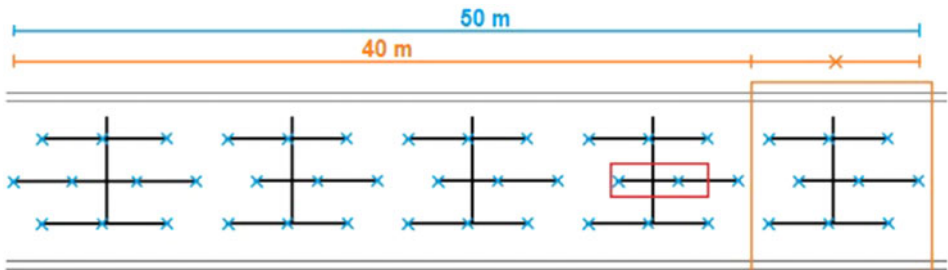


**Figure 7. Nozzle positioning, zone distance and fire location (red). Note Test 6 is based on fire at end of zone omitting  $\times$  zone of deluge piping as shown above (Color figure online).**

#### 2.4. Heat Release Rate Estimate

There are a few methods of heat release rate measurement. The most common are by using the measured mass loss rate and by using oxygen depletion calorimetry, where the heat release rate is based on the amount of oxygen consumed.

In fire tests with a suppression system, the use of the mass loss rate is not possible because water flow during activation of the suppression system will disturb the measurement of mass loss of the fire source and this will affect the accuracy of the heat release rate measurement.

The method based on oxygen depletion uses the known amount of energy produced per unit of oxygen consumed (for a specific group of combustibles). Using this method, there are three different techniques: use of the oxygen measurement alone (method 1) or oxygen with carbon dioxide (method 2) or oxygen along with both carbon dioxide and carbon monoxide (method 3) measurements, which are

then input to equations. The accuracy of the latter three methods increases with the number of the method [6].

In this work, the heat release rate estimate is based on the oxygen depletion method, where besides oxygen concentration, carbon monoxide and carbon dioxide production are also measured to increase the accuracy of the HRR estimate.

The heat release rate is calculated according to the “basic equations” 1 and 2 given by Dlugogorski et al. [6]. The “basic equations” take into account the influence of the water vapor content and correspond mathematically to the equations derived by Parker [7]. In contrast to the equations of [7] however, the “basic equations” do not require calculation of the molecular flow rate, nor the humidity of the incoming air and are therefore easier to use.

For convenience the “basic equations” [6] are given below.

$$\dot{q} = n_{total}^e (1 - X_{H_2O}^e) \left[ 0.5(E - E^{co})X_{co}^{e,d} + E \left( X_{o_2}^{i,d} \frac{1 - X_{o_2}^{e,d} - X_{co_2}^{e,d} - X_{co}^{e,d}}{1 - X_{o_2}^{i,d} - X_{co_2}^{i,d}} - X_{o_2}^{e,d} \right) \right], \quad (1)$$

where the total molar flow for an ideal gas is:

$$n_{total}^e = m_{air}^{e,d} / \left( M_{total}^e \times M_{air}^{i,d} \right)^{0.5}. \quad (2)$$

As the total molecular weight  $M_{total}^e$  differs from  $M_{air}^{i,d}$ , Eq. 2 is used to compute  $n_{total}^e$ .

$$M_{total}^e = X_{H_2O}^e M_{H_2O} + (1 - X_{H_2O}^e) \left( X_{N_2}^{e,d} M_{N_2} + X_{O_2}^{e,d} M_{O_2} + X_{CO_2}^{e,d} M_{CO_2} + X_{CO}^{e,d} M_{CO} \right). \quad (3)$$

The ‘exhaust’ molar flow rates are determined from the measured velocities, temperatures and mole fractions 170 m downstream from the fire location. The measured velocities, temperatures and concentrations at positions M16, M26 and M36 (Figures 2a, b, 10 and 11) are used to establish the contribution of the heat release rate at the lower 2/3 part of the tunnel cross section. The remaining portion of the heat release rate estimate at the upper 1/3 part of the tunnel cross section is measured at positions M46 and M51 (Figure 2b, 11) in the tunnel. The measured molar fractions of O<sub>2</sub>, CO, CO<sub>2</sub> and water vapor at position M46, M26 (Figure 11) are used for the heat release rate estimate in the upper and lower part of the tunnel. The molar fractions of O<sub>2</sub> and CO<sub>2</sub> of the incoming air are set at 0.2095 and 0.00041 respectively.

The molar fraction of N<sub>2</sub> at the exhaust is determined from the following equation:

$$X_{N_2}^{e,d} = 1 - X_{O_2}^{e,d} - X_{CO_2}^{e,d} - X_{CO}^{e,d}. \quad (4)$$

Given the uncertainty in the measurements and the observed velocity, temperature and concentration profiles at D170 M a relative error of approximately ±10% in

the calculated value of the heat release rate is expected. An exact error estimation is outside the scope of the research, but in line with general error estimates for this type of measurement.

Several checks have been made to minimize the error in the concentration measurements based on the known relation between  $\text{CO}_2$  production and  $\text{O}_2$  depletion. A significant part of the error is caused by the non-uniform velocity and concentration profiles at D170.

### 2.5. Results of Fire Test

As the information obtained from this fire test program is substantial, only the information on the heat release rate for all the tests (Figures 8, 9) and parameters of velocity, temperature,  $\text{O}_2$ ,  $\text{CO}$ ,  $\text{CO}_2$  and heat flux for Test 4 and 7 are presented (Figures 10, 11, 12). The information in Fire Test 4 and 7 provides a basis for comparing the condition in the tunnel with and without deluge system operation.

The photographs of these fire tests are also shown in Figure 13 and their peak HRR, calorific energy are summaries in Table 2 respectively.

## 3. Discussion of Fire Test Results

Observations from these large scale fire tests show (Figure 8) that there is a significant reduction in heat release rate between the fire tests with deluge operating at 4 min (Test 1 to 5) as compared to the fire tests with delayed operation at 8 min (Test 6) or a free burning condition (Test 7). Upon activation of the deluge sys-

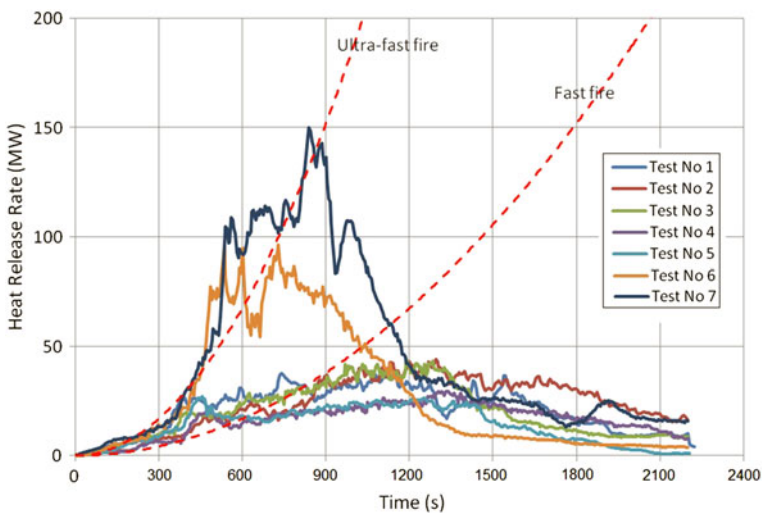


**Figure 8. HRR estimate for large-scale test of HGV fire with and without (Test 7) fire suppression. Note Test 1 to 5—deluge operates at 4 min; Test 6—deluge operates at 8 min; Test 7—free burning.**

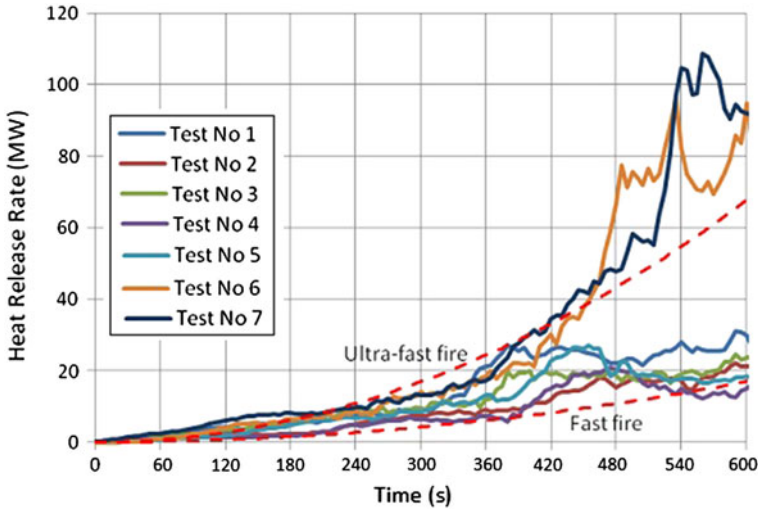
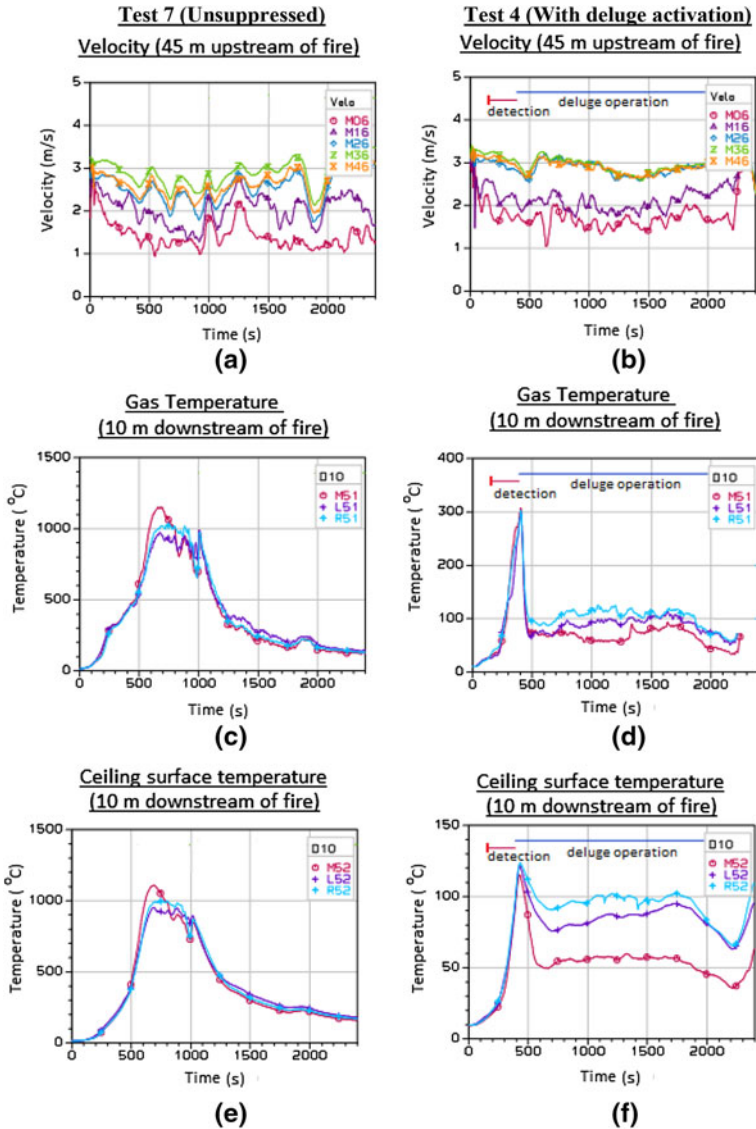


**Figure 9. Initial growth rate for large-scale test of HGV fire.**

tem, the peak heat release rates of this group of tests (Test 1 to 5) are reduced by 70% to 81% as compared with the fire (Test 7) without deluge operation. Based on the test schedule result in Table 2, peak heat release rates varying between 27 MW and 44 MW were obtained for scenarios with deluge activation at 4 min. In Test 6 with delayed activation, the peak heat release rate reduction is significantly less (reduced by 35%). The decrease in deluge system performance in Test 6 is probably not only caused by the delayed activation but also due to damage to the nozzles above the fire. Operating the deluge system at the early stage of the fire development is critical as it helps to reduce the severity of the fire during the growth phase.

All the tests with deluge operation within 4 min are controlled below the peak heat release rate of 50 MW. It appears that a fast to ultra-fast growth rate was observed during the first 7 min of the fire development for all the tests. The fire growth rate for Test 6 and 7 increased even more rapidly after 7 min when intervention from the deluge system is not applied (Figure 9). In the unsuppressed test in Test 7, it was observed that there is an increase in heat release rate from the steady 110 MW to 150 MW suddenly at time 12.8 min. This is attributed to the collapse of pallets stacks during the burning process as a large amount of the pallets surface area is exposed to the fire. Without a suppression system, this further promotes rapid burning and results in a sudden heat release rate increase.

The following paragraphs discuss the fire test information for Fire Test 4 and 7 and provide a basis for comparing the condition in the tunnel with and without deluge system operation. Figure 10a and b give a time base event of the velocity profile at the upstream of the fire for Test 4 and 7. At the upper cross section of the tunnel (e.g. M26, M36 and M46), an average of 3 m/s is maintained with lower velocities experienced at the lower cross section of the tunnel (e.g. M06 and



Note: a)  $\uparrow$  detection at 60°C, b)  $\text{—}$  system activates after 4 min, c)  $\text{—}$  deluge operation

**Figure 10. Velocity, gas and ceiling temperature (Color figure online).**

M16). This is due to obstacles and a person moving in the lower part of the tunnel.

The gas temperature and tunnel ceiling temperature 10 m downstream of the fire (Figure 10) were measured and presented for the unsuppressed fire—Test 7

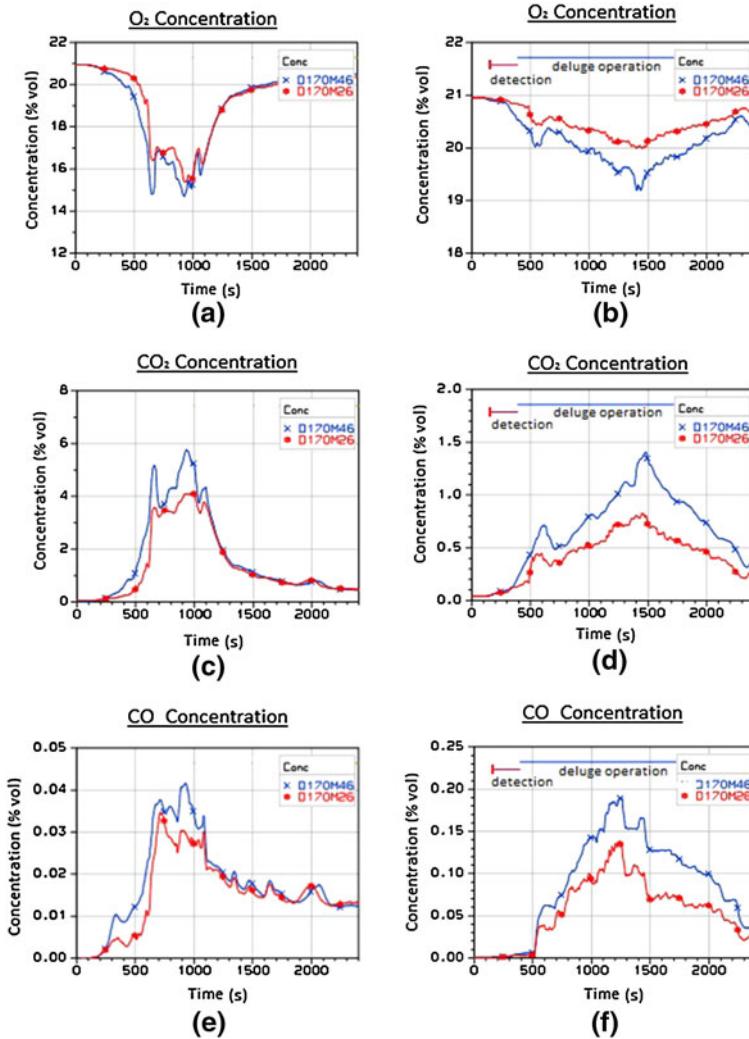


**Figure 11. O<sub>2</sub>, CO<sub>2</sub> and CO concentration (Color figure online).**

and with deluge activation—Test 4 respectively. In Test 7, a rapid temperature increase was observed until 650 s at 1,150 °C, with a steady decrease thereafter (Figure 10c). In the suppression test (Test 4), a rapid increase in temperature was also observed at the growth phase of the fire until the activation of the deluge system at 400 s with an immediate sharp reduction in temperature (Figure 10d). Early activation and a correctly operating deluge suppression system can help to limit the temperature development in the tunnel structure, therefore reducing the risk of structure collapse. This is evident from the results shown in Test 7 and Test 4 where a maximum ceiling surface temperature of 1,100 °C (10 m downstream of fire) was recorded for the unsuppressed test (Figure 10e) compared to a

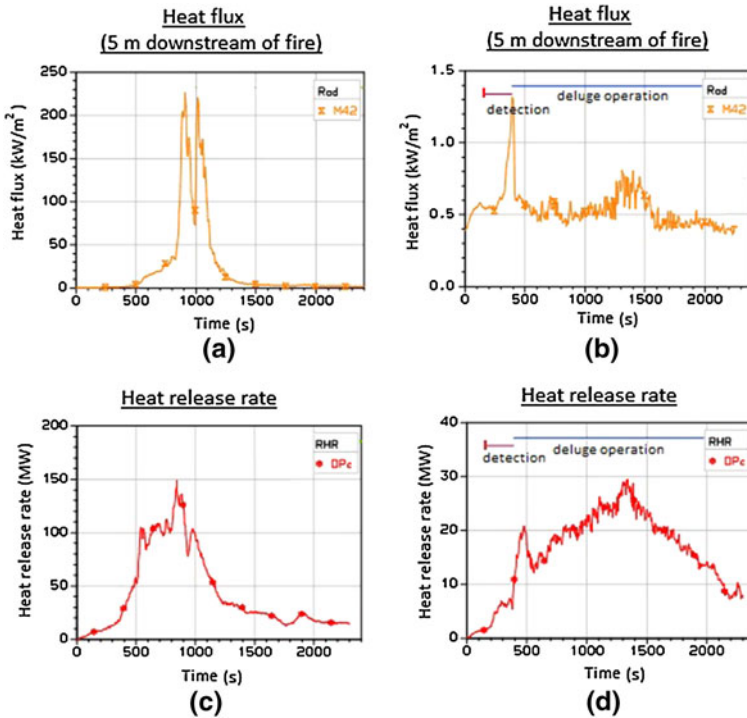


**Figure 12. Heat release rate and heat flux for Test No. 7 (left) and No. 4 (right) (Color figure online).**

reduction in ceiling surface tunnel temperature to 120 °C (10 m downstream of fire) for the suppressed test (Figure 10f).

The influence of the suppression system on CO production is significant (Figure 11e, f). The fire test with suppression (Test 4) results in about a five times higher CO concentration at a 2.6 m height, 170 m downstream from the fire when the deluge system is operated than for the unsuppressed test (Test 7). This means an increase in CO yield of about 20 times, because the suppressed heat release rate is about 4 times less than the unsuppressed heat release rate and the ventilations rates are about the same. Similar high CO concentrations and increased CO yields are found in all suppressed tests, indicating incomplete combustion due to the water suppression. High CO concentrations have also been reported for 100 MW fire tests with a water mist system in the Runehamar tunnel [8]. In general, high CO concentrations have not been frequently reported, because of the lack of non-commercial CO-measurements for sprinklered tunnel fires with high heat release rates.

The low CO concentrations in Test 7 indicate that the supply of fresh air was not significantly obstructed by the cover in the free burning situation. It also indicates that the high CO values were not caused by insufficient mechanical ventilation.



**Figure 13. Photographs of the fire tests.**

**Table 2**  
**Peak HRR and Calorific Energy**

Test	Discharge density (mm/min)	Activation time (min)	Time to peak (min)	Peak HRR (MW)	Integrated calorific energy (GJ)
1	12	4	12.3	37.7	46.6
2	8	4	21.6	44.1	52.7
3	12	4	19.8	44.2	44.5
4	12	4	21.8	29.5	35.9
5	12	4	7.6	27.1	30.2
6	12	8	8.9	96.5	61.6
7	n.a.	n.a.	14	150	99.2

The ratio between  $O_2$  depletion and  $CO_2$  production is typically 1.1 for wood and 1.5 for plastics. The value of this ratio in the tests can be derived from Figure 11a and c for Test 7 and in Figure 11b and d for Test 4. A ratio of 1.2 is found for Test 7 and 1.3 for Test 4. In general a ratio between 1.2 and 1.3 is found for all tests. These ratios are in accord with the values mentioned above and underscore the assumed accuracy of the heat release measurements.

In Test 4 with suppression activated at 4 min after detection, the heat flux level 5 m downstream of the fire was maintained at a relatively low value of  $1.3 \text{ kW/m}^2$  (Figure 12b) compared to the unsuppressed test of  $220 \text{ kW/m}^2$  at its peak (Figure 12a). Unlike Test 4, the target pallet stack located 5 m downstream of the fire was ignited in Test 7 since the minimum ignition heat flux for wood material is around  $10 \text{ kW/m}^2$ .



In Figure 12c and d, a clear distinction can be seen between the heat release rate for the suppression test (Test 4) with a 4 min activation and without suppression (Test 7). Based on the tests results, a design fire size of 50 MW is sufficient when the deluge suppression system is activated within 4 min with a 12 mm/min discharge density. However, the use of a design fire size of 100 MW is more appropriate when the possibility of late activation (8 min—Test 6) is to be taken into account.

## 4. Conclusions

This article describes the test setup and results of the large scale fire test program for road tunnels with deluge system operation. The calculation of the heat release rate of heavy goods-vehicle fires in a tunnel with and without deluge system operation is presented. Peak heat release rates of 27.1 MW to 44.2 MW (deluge operate at 4 min), 96.5 MW (deluge operate at 8 min) and 150 MW (no deluge intervention) were measured in these fire tests. The activation of the deluge system at the early phase of the fire development (within 4 min) is critical as it helps to reduce the severity of the fire development during the growth phase, which is particularly true for burning HGVs carrying material with a high energy content. The influence of the suppression system on CO production is significant, because high CO concentrations and increased CO yields were found in the suppressed tests, indicating incomplete combustion due to the water suppression.

## Acknowledgments

The personnel at Efectis BV, Aquasys and TST are gratefully acknowledged for their work in performing the large-scale tunnel tests at TST tunnel in Spain together with FSSD (Mr Heng Chai Liang, Major Chong Kim Yuan).

## Funding

The fire tests were funded by the Land Transport Authority (LTA) in Singapore with the support from the Singapore Civil Defence Force (SCDF).

## References

1. Ingason H, Lönnemark A (2005) Heat release rates from heavy goods vehicle trailer fires in tunnels. *Fire Saf J* 40:646–668
2. Studiengesellschaft Stahlanwendung e.V Dusseldorf (1995) Fire in transport tunnels—report on full-scale tests, EUREKA-Project EU 499: FIRETUN
3. Tunnel safety testing (TST) Web-site <http://www.tunneltest.com/ingles/tunelensayo.php>. Accessed 13 July 2012
4. Implementation of vehicle immobiliser system in Phase 2 of the Hazmat Transport Vehicle Tracking System, Singapore Civil Defence Force, Jan 2007

5. Singapore Gazette, Road Traffic Act 2006, Chapter 276, Sections 114 and 140, Road Traffic Expressway Traffic Rules, June 2006
6. Dlugogorski BZ, Mawhinney JR, Huu Duc V (1994) The measurement of heat release rates by oxygen consumption calorimetry in fires under suppression. *Fire Saf Sci* 4:877–888. doi:[10.3801/IAFSS.FSS.4-877](https://doi.org/10.3801/IAFSS.FSS.4-877)
7. Parker WJ (1982) Calculation of the heat release rate by oxygen consumption for various applications, U.S. Department of Commerce, National Bureau of Standards, NBSIR 81-2427, 1–38, Feb 1982
8. Meeussen VJA et al (2008) The effect of a water mist system on large-scale tunnel fires. Proceedings of the ITA COSUF workshop on safety and security of railway and metro tunnels, Graz, Austria, 23 Apr 2008